Science Advances
AAAS

advances.sciencemag.org/cgi/content/full/6/46/eabc3099/DC1

Supplementary Materials for

The structure-function relationship of oncogenic LMTK3

Angeliki Ditsiou, Chiara Cilibrasi, Nikiana Simigdala, Athanasios Papakyriakou, Leanne Milton-Harris, Viviana Vella, Joanne E. Nettleship, Jae Ho Lo, Shivani Soni, Goar Smbatyan, Panagiota Ntavelou, Teresa Gagliano, Maria Chiara Iachini, Sahir Khurshid, Thomas Simon, Lihong Zhou, Storm Hassell-Hart, Philip Carter, Laurence H. Pearl, Robin L. Owen, Raymond J. Owens, S. Mark Roe, Naomi E. Chayen, Heinz-Josef Lenz, John Spencer, Chrisostomos Prodromou, Apostolos Klinakis, Justin Stebbing, Georgios Giamas*,

*Corresponding author. Email: g.giamas@sussex.ac.uk

Published 13 November 2020, *Sci. Adv.* **6**, eabc3099 (2020)
DOI: 10.1126/sciadv.abc3099

The PDF file includes:

Other Supplementary Material for this manuscript includes the following:

(available at advances.sciencemag.org/cgi/content/full/6/46/eabc3099/DC1)

Supplementary materials and methods

Cell lines and cloning

ERα$^+$ (MCF7, T47D), TNBC (MDA-MB-231, BT549) and non- transformed MCF12A cell lines were purchased from ATCC. MCF7 and MDA-MB-231 cells were maintained in low glucose DMEM (Sigma Aldrich, #D6046-500ML) supplemented with 10% FBS (Sigma Aldrich, #F7524-500ML) and 1% Penicillin/Streptomycin (Sigma-Aldrich, #P0781-100ML). T47D and BT549 cells were maintained in RPMI-1640 medium (Sigma Aldrich, #R5886-500ML) supplemented with 10% FBS (Sigma Aldrich, #F7524-500ML) and 1% L-glutamine/Penicillin/Streptomycin solution (Sigma-Aldrich, #G1146-100ML). MCF7/LMTK3 cell line stably overexpressing LMTK3 has been described before (*6*). MCF12A cells were maintained in Cascade Biologics medium 171 (Gibco, #M-171-500) supplemented with 10% FBS (Sigma Aldrich, #F7524-500ML), 1% L-Glutamine/Penicillin/Streptomycin (Sigma Aldrich, #G1146-100ML), 1% mammary epithelial growth supplement (Thermo Fisher Scientific, #S0155) and 100 ng/ml cholera toxin from Vibrio cholerae (Sigma Aldrich, #C8052-5MG). The FDCP1 parental cell line was cultured in RPMI-1640 medium (Sigma- Aldrich, #R5886-500ML) supplemented with 10% heat-inactivated FBS (30 minutes at 56°C) (Sigma-Aldrich, #F7524- 500ML), 1% L-glutamine / penicillin / streptomycin (Sigma-Aldrich, #G1146-100ML), 0.5 μg/mL puromycin (Gibco, #A1113803) and 10 ng/mL recombinant mouse interleukin 3 (IL3) (Genscript, #P01586), while the LMTK3- transformed FDCP1 cells didn't require IL3 for their growth.

Parental IL3-dependent FDCP1 and transformed FDCP1-LMTK3 cells were purchased from Advanced Cellular Dynamics, Inc. To create the FDCP1-LMTK3 cell line, FDCP1 cells were transduced with a pACD320 retroviral vector encoding the BCR (breakpoint cluster region) protein fused to FLAG epitope-tagged LMTK3 gene, which encompasses aa 134-444 (kinase domain). This fusion-donor approach is employed because different kinases often demonstrate preferential transformation capacity based on their ability to dimerize, which depends on the specific fusion partner deployed (*70*) (fusions with other proteins including NPM, TPR, bTEL and nTEL did not result in high transactivation of LMTK3 as the one observed with BCR). The oncogene transformed derivative cells are cytokine-independent and rely on the constitutive expression of catalytically active LMTK3 for their survival and proliferation. All the cells were incubated at 37°C with 5% CO_2.

Reagents

MG-132 (#474790) was purchased from Millipore and resuspended in DMSO (Millipore, # D/4125/PB08). Cyclohexamide (# 357420010) was purchased from Thermo Fisher Scientific and resuspended in DMSO (Millipore, #D/4125/PB08). Geldanamycin (#HY-15230) and NVP-AUY922 (#HY-10215/CS-0136) were purchased from MedChemExpress and resuspended in DMSO (Millipore, #D/4125/PB08, UK). Recombinant human HSP27 protein (#ab48740) was purchased from Abcam. ERα (1:1000, #8644), phospho-HSP27 (Ser15) (1:1000, #2404), phospho-HSP27 (Ser82) (1:1000, # 9709), HSP27 (1:1000, #3936), BCL2 (1:1000, # 2870), BCL-XL (1:1000, #2764), cleaved-PARP

(1:1000, cat. no. 5625), His-Tag (D3I1O) XP® (#12698), Flag (1:50, #8146), CDK4 (1:1000, #12790), HSP90 (1:1000, ca#4877) and CDC37 (1:1000, #4793) antibodies as well as anti-rabbit IgG (1:5000, #7074P2) and anti-mouse IgG (1:5000, #7076P2) HRP-linked antibodies were purchased from Cell signaling. HSP70 (1:1000, #EXOAB-Hsp70A-1) was purchased from System biosciences and HIPK2 (1:1000, #BS60320) was purchased from Bioworld Technology. Phosphor-DYRK1/A (Tyr 321/273; 1:1000, #12497) and phospho-TRKA (Tyr 680/681; 1:1000, #11904) were purchased from SAB, FLAG antibody (1:1000, #F7425) was purchased from Sigma Aldrich, GAPDH (1μg/ml, #39-8600) was purchased from Thermo Fisher Scientific, while TRKA (1:1000, #A01404), β-actin (0.1 μg/ml, #A00702-100) and α-tubulin (1:1000, #A01410-100) were purchased from GenScript. CLK2 (1:1000, #A7885), DYRK1A (1:1000, #A0595) and IRAK4 (1:1000, cat. no. A6208) were purchased from ABClonal. A Sigma Aldrich antibody (1:500, #WH0114783M2) was used to detect total LMTK3, while an Abcam antibody (1:500, #110516) was used to detect its kinase domain. pCMV6-LMTK3 overexpressing plasmid (#RC223140) and the pCMV6 empty vector (#PS100001) were purchased from Origene. All the other reagents, if not otherwise specified, were purchased from Thermo Fisher Scientific.

Expression and purification of GST fusion proteins

Wild-type GST-HSP27, mutants GST-HSP27/Ser15Ala and GST-HSP27/Ser82Ala proteins were expressed in transformed BL21 (DE3) cells (New England Biolabs, cat. no. C2527I) in Luria Broth media. Protein expression was induced with addition of 0.5 mM IPTG at 20 °C overnight. Cells were resuspended in lysis buffer containing 20 mM Tris pH 8.0, 200 mM NaCl, 10% glycerol, 0.5% NP-40, 1 mM DTT, 1 mM EDTA and protease inhibitors (Roche Diagnostics GmbH, cat. no. 11697498001) and were sonicated using an MSE Soniprep 150. Lysates were affinity purified using glutathione agarose (GE Healthcare, cat. no. 17-5279-01), eluting in 20 mM reduced glutathione (Duchefa Biochemie, cat. no. 70-18-8) in 50 mM Tris pH 8.0, 200mM NaCl and 0,1% 2-mercaptoethanol. Fractions were analysed by SDS-PAGE and Coomassie staining. Proteins were concentrated to 1.0 mg/mL and snap frozen for storage at -80 °C. All purification steps were carried out at 4 °C.

PepChip analysis

PepChip microarray slides are spotted with a duplicate set of 192 peptides that contain experimentally verified phosphorylation sites for different protein kinases and their original surrounding residues. Each peptide consists of 8-9 amino acids, of which approximately the central position corresponds to the putative phosphorylation site (Ser, Thr or Tyr residue). For incubation of the PepChip slide, an *in vitro* kinase assay was performed, using 2μg of wt LMTK3cat mixed with 5 μl of ^{32}P γ-ATP. The mix was brought onto a cover slide, after which the PepChip was posed over the sample and turned around, following incubation for 4 h at 30 °C in a closed wet box to prevent drying of the slide. The cover slide was rinsed off the PepChip with 50 mM Tris, pH 7.5, 150 mM NaCl, 0.02% Tween 20 (TBST) and the PepChip was then washed twice with 2 M NaCl, once with 2 M urea, twice with 10% SDS, and three

times with MilliQ water in a washing tube. The intensity of phosphorylated substrates was then quantified using standard autoradiography.

Western blotting

Protein lysates were extracted using RIPA buffer (Sigma Aldrich, cat. no. R0278-50ML) including fresh protease and phosphatase inhibitors (Roche Diagnostics GmbH, cat. no. 11697498001 & cat. no. 4906845001). Briefly, protein concentration of the lysates was determined using the Pierce BCA protein assay kit (ThermoFisher Scientific, cat. no. 23227) and 30/50 µg of protein extract was resolved on SDS/PAGE gels (GenScript, cat. no. M42012 & cat. no. M00653). Proteins were then transferred onto a nitrocellulose blotting membrane (Thermo Fisher Scientific, cat. no. IB23001) using the iBlot 2 dry blotting system (Thermo Fisher Scientific, cat. no. IB21001). The membranes were blocked in TBS containing 0.1% (v/v) Tween 20 and 5% (w/v) non-fat milk or 5% (w/v) BSA (VWR Life Science, cat. no. 421501J) for 1 hour before being incubated with the primary antibodies overnight at 4°C. HRP-conjugated secondary anti-rabbit (1:5000, Cell Signaling, cat. no. 7074P2) or anti-mouse (1:5000, Cell Signaling, cat. no. 7076P2) antibodies were used. Chemiluminescent detection was performed using the SuperSignal West Pico PLUS Chemiluminescent Substrate (Thermo Fisher Scientific, cat. no. 34577). Emission was captured using the UVP ChemStudio Imaging Systems (Analityk Jena).

Co-immunoprecipitation

To examine kinase-chaperone interactions, proteins were extracted and co-immunoprecipitated from 350 µg protein lysate in 150µL modified RIPA buffer [50 mM Tris-HCl pH 7.5, 150 mM NaCl, 1% sodium deoxycholate, 1% NP-40 alternative, 0.02% SDS containing protease and phosphatase inhibitors (Roche Diagnostics GmbH, #11697498001 & #4906845001)] with 1:50 anti-Flag antibody (Cell signaling, #8146) or 1:50 anti-CDC37 antibody (Cell signaling, #4793) overnight at 4°C. Antigen-antibody complexes were purified using Protein G resin (Genscript, #L00209), which was pre-blocked with 1% BSA-RIPA buffer for 4 hours at 4°C. After washing of the beads, bound proteins were eluted by boiling in 1×SDS gel loading buffer and analyzed by immunoblotting.

Cell viability assay

Mammalian cells were cultured at 3000 cells/well in 96-well plates (Corning, #3603). Cell viability was assessed using the CellTiter-Glo luminescent cell viability assay (Promega, #G7572), as previously described (Stebbing et al., 2018). FDCP1 and LMTK3-transformed FDCP1 cells were plated at 5000 cells/well in 384-well plates (Aurora Biotechnologies, cat. no. 2030-10200). After 24 hours, cells were treated with increasing concentrations of a panel of kinase inhibitors for 48 hours. Control cells were treated with DMSO, at the same dilution as the highest concentration of treatment. After incubation, CellTiter-Glo reagent was added to each well and luminescence was recorded with the GloMax®-Multi detection system (Promega) as described above.

Cell death and apoptosis

Cells were treated with increasing concentrations of C28 for 72 h. After collection, cells were stained with the Muse Annexin V Dead Cell Kit according to the manufacturer's protocol (Millipore, #MCH100105). Cells were then analyzed using the Muse Cell Analyzer (Millipore).

LMTK3 silencing and overexpression

Cells were transfected with a pool of 3 LMTK3 siRNAs (#s41588, #s41589, #s415890 Ambion) or scramble control (#4390843, Ambion) using the 4D-Nucleofector™ System (LONZA), following the manufacturer's instructions. Briefly, $5x10^5$ cells were resuspended in 20 µl of complete buffer SE (Lonza, #PBC1-00675) and 300 nM siRNA were added prior electroporation. Cells were then seeded in warm complete medium. For overexpression, $3x10^5$ cells were seeded per well in a 6-well plate. Cells were then transfected with 2 µg of pCMV6-LMTK3 plasmid encoding full-length LMTK3 (Origene, #RC223140) or pCMV6 vector (Origene, #PS100001) using Fugene HD transfection reagent (Promega, #E2311), following the manufacturer's instructions.

Protein digestion and phosphopeptide enrichment

FASP procedure was performed as previously described (71). In all, 500 ul FASP 1 (8 M urea, 20mM DDT in 100mM Tris/HCL pH 8.5) was added to B2 mg protein lysate to dilute SDS concentration and transferred to a Vivacon 500, 30k MWCO HY filter from Sartorius Stedim Biotech (Epsom, UK). The sample was buffer exchanged using FASP 1 several times by spinning the tube at 7000 g to remove detergents. The protein lysate was concentrated by centrifugation and diluted in FASP 2 (100 mM Tris/HCl pH 8.5) ready for trypsin digestion. The sample was reduced using 50 mM fresh IAA in FASP 2 in the dark for 30 min. Lysates were spun down to remove excess IAA and buffer exchanged into FASP 3 (100 mM triethyl ammonium bicarbonate). Trypsin was dissolved in FASP 3 to give a 1 : 200 enzyme to protein ratio and added in a volume of at least 100 ml for 4–6 h. This was repeated with fresh trypsin for a further overnight incubation. Lysates were spun down and washed with 0.5 M NaCl and 150 ml 10% TFA added to reduce the pH. A standard desalting procedure was used (72).

Hydrophilic interaction chromatography (HILIC) fractionation

A TSKgel Amide-80 separation column with a TSKgel Amide guard column was used for HILIC separation of FASP peptides. Buffer A: 80% ACN, 0.1% formic acid and buffer B: 0.1% formic acid was used for the gradient at a flow rate of 0.6 mJ min–1. The sample was separated into 45 fractions, collected 2 mins per vial and dried using a speed vac. TiO2 enrichment was performed as previously described (72). TiO2 beads were washed and re-suspended in buffer B at 50 mg ml –1 and added to tubes to give 1 mg per tube. The sample was re-suspended in loading buffer, added to beads and incubated at RT for 20 min. After washing, using buffers A and B samples were eluted using aliquots of 0.5% NH4OH. Elutions were pooled and 10 ml of 20% FA added to adjust the pH. Samples were dried and re-suspended in 1% FA.

Mass spectrometry methods

Trypsin-digested peptides were separated using an Ultimate 3000 RSLC nanoflow LC system from Thermo Scientific (Cramlington, UK). On average 0.5 mg was loaded with a constant flow of 5 ml min–1 onto an Acclaim PepMap100 nanoViper C18 trap column (100 mm inner-diameter, 2 cm; Thermo Scientific). After trap enrichment, peptides were eluted onto an Acclaim PepMap RSLC nanoViper, C18 column (75 mm, 15 cm; Thermo Scientific) with a linear gradient of 2–40% solvent B (80% acetonitrile with 0.08% formic acid) over 65 min with a constant flow of 300 nl min–1. The HPLC system was coupled to a linear ion trap Orbitrap hybrid mass spectrometer (LTQ-Orbitrap Velos, Thermo Scientific) via a nano electrospray ion source (Thermo Scientific). The spray voltage was set to 1.2 kV, and the temperature of the heated capillary was set to 250 1C. Fullscan MS survey spectra (m/z 335–1800) in profile mode were acquired in the Orbitrap with a resolution of 60 000 after accumulation of 1 000 000 ions. The 15 most intense peptide ions from the preview scan in the Orbitrap were fragmented by collision-induced dissociation (normalised collision energy, 35%; activation Q, 0.250; and activation time, 10 ms) in the LTQ after the accumulation of 10 000 ions. Maximal filling times were 1000 ms for the full scans and 150 ms for the MS/MS scans. Precursor ion charge state screening was enabled, and all unassigned charge states as well as singly charged species were rejected. The lock mass option was enabled for survey scans to improve mass accuracy. Data were acquired using the Xcalibur software from Thermo Scientific.

Quantification and bioinformatics analysis

The raw mass spectrometric data files were collated into a single quantitated dataset using MaxQuant (version 1.2.2.5) and the Andromeda search engine software and the “heavy” to “light” peptide ratios (H/L) were subsequently determined, as shown in Table S2. Enzyme specificity was set to that of trypsin, allowing for cleavage N-terminal to proline residues and between aspartic acid and proline residues. Other parameters used were: (i) variable modifications, methionine oxidation, protein N-acetylation, gln→pyro-glu, Phospho(STY); (ii) fixed modifications, cysteine carbamidomethylation; (iii) database: target-decoy human MaxQuant (ipi.HUMAN.v3.68); (iv) heavy labels, R10K8; (v) MS/MS tolerance: FTMS- 10ppm , ITMS- 0.6 Da; (vi) maximum peptide length, 6; (vii) maximum missed cleavages, 2; (viii) maximum of labeled amino acids, 3; and (ix) false discovery rate, 1%. Peptide ratios were calculated for each arginine- and/or lysine-containing peptide as the peak area of labeled arginine/lysine divided by the peak area of non-labeled arginine/lysine for each single-scan mass spectrum. Peptide ratios for all arginine- and lysine-containing peptides sequenced for each protein were averaged. Data is normalized using 1/median ratio value for each identified protein group per labelled sample.

Supplementary Figures

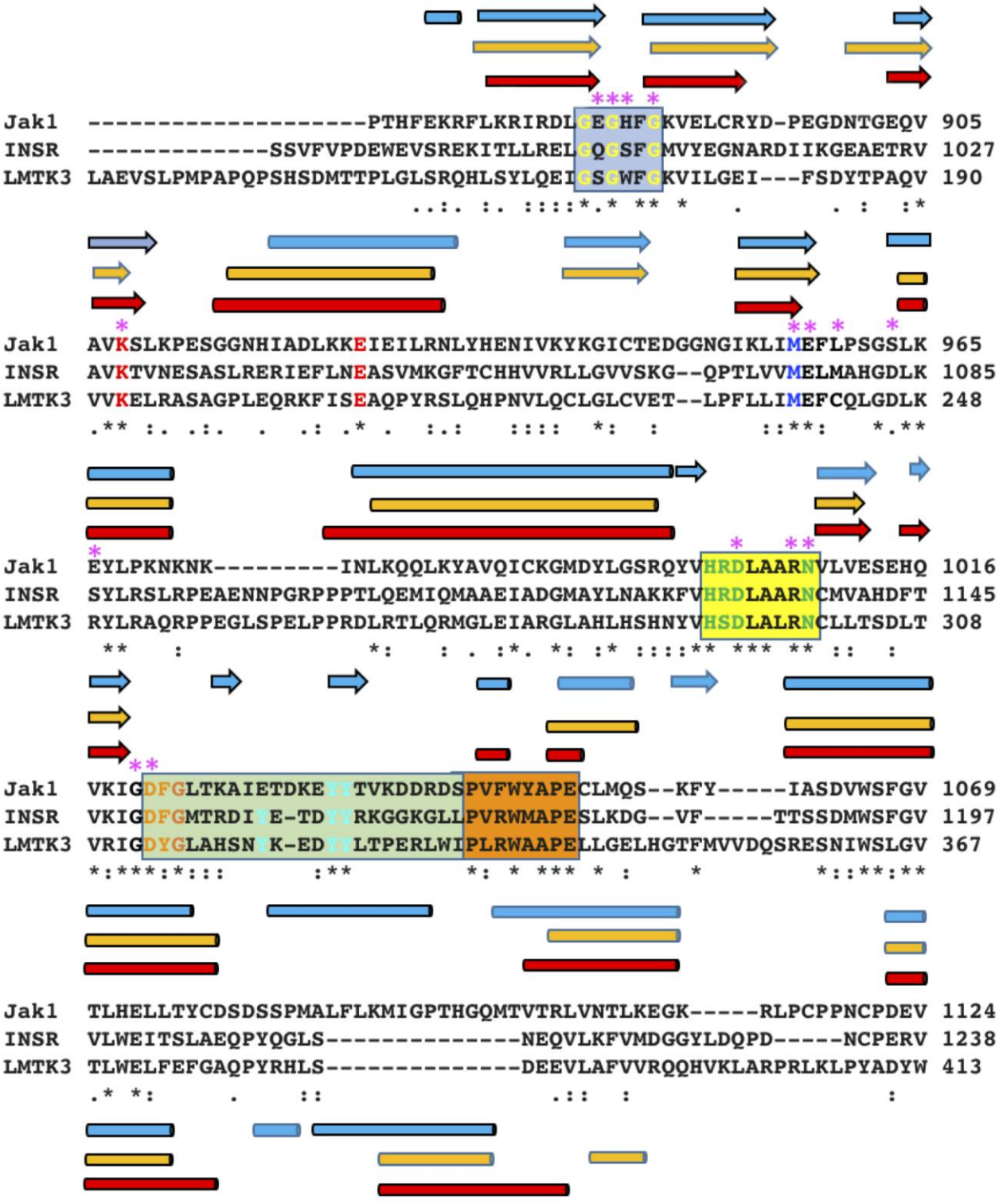

Figure S1. Sequence alignment showing the main features of the kinase domain.

The DYG (normally DFG) and APE motifs define the extent of the activation segment, which consists of the activation- and P+1- loop. Colored arrows represent beta-strands while colored cylinders represent helices (Cyan: JAK1; Orange: INSR; Red: LMTK3). *Blue box*: glycine–rich loop with glycine coloured yellow. *Blue residue*: gatekeeper methionine residue. *Red residues*: amino acids involved in the lysine-glutamate salt bridge. *Yellow box:* catalytic loop containing the HXD motif and Asn300 (green residues). *Olive box*: activation loop containing the DXG motif (orange residues) and potential phosphotyrosine residues (cyan residues). *Orange box*: the P+1 loop. *Pink asterisk*: residues involved in ATP binding. *Black symbols* (.), (:) and (*): represent conservation as determined by Clustal Omega (*73*).

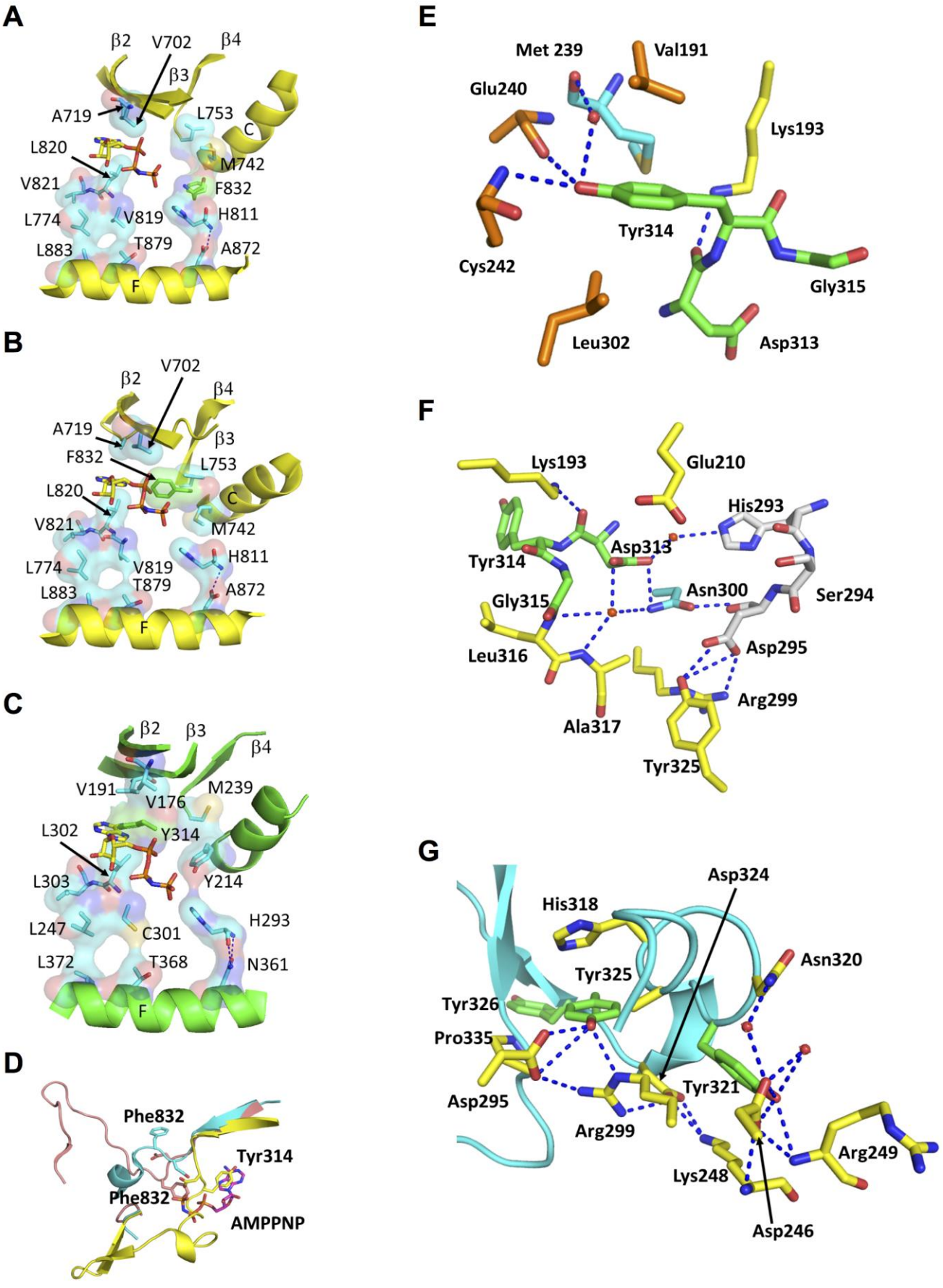
A
β2
V702
β4
β3
A719
L753
C
L820
M742
V821
F832
L774
V819
H811
L883
T879
A872
F
B
V702
β2
β4
A719
β3
F832
L753
L820
C
V821
M742
L774
V819
H811
L883
T879
A872
F
C
β2
β3
β4
V191
M239
V176
L302
Y314
L303
Y214
L247
C301
H293
L372
T368
N361
F
D
Phe832
Tyr314
Phe832
AMPPNP
E
Met 239
Val191
Glu240
Lys193
Tyr314
Cys242
Gly315
Leu302
Asp313
F
Lys193
Glu210
His293
Asp313
Tyr314
Asn300
Ser294
Gly315
Asp295
Leu316
Arg299
Ala317
Tyr325
G
Asp324
His318
Asn320
Tyr325
Tyr326
Pro335
Tyr321
Asp295
Arg299
Arg249
Lys248
Asp246

Figure S2. Modulation of C- and R-spine integrity by the DXG motif and Pymol cartoon showing packing interactions of the DYG motif tyrosine residue, interactions of the HSD and DYG motif and phospho-tyrosine packing.

(A) Key residues forming the C- and R-spine of active EGFR (PDB 5CNO). The phenylalanine residue (Phe832, green sticks) of the DFG motif packs between His 811 and Met 742 and completes the R-spine (right hand space fill), while the adenine ring of AMPPNP (gold sticks) completes the C-spine. The R-spine, is a series of hydrophobic residues that connect essential elements required for catalysis to the F-helix, while the ATP helps to complete the C-spine, a series of residues that connect the F-helix to the N-terminal lobe (*26, 27*). **(B)** In the inactive state of the EGFR kinase (PDB 2RF9) the phenylalanine residue (Phe832, green sticks) of the DFG motif is positioned as such that AMPPNP bonding is incompatible and neither the C- nor R-spine remain intact. **(C)** The inactive state of LMTK3. Tyr314 (green sticks) of the DYG motif is positioned as such that it prevents AMPPNP binding but maintains the integrity of the C-spine (left hand space fill). Thus, although EGFR and LMTK3 show homology the detailed mechanism by which they achieve an inactive state and prevent ATP binding differs in detail. The C-helix of the C-terminal lobe and the F-helix and beta-strand 2, 3 and 4 of the N-lobe of the kinase are shown as arrows or helices. Blue dashes, hydrogen bonds. **(D)** Active and inactive positions of the DXG motif. Superimposition of inactive (salmon, PDB 2RF9) and active EGFR (cyan, PDB 5CNO) structures with inactive LMTK3 (yellow, PDB 6SEQ). In the inactive structure of EGFR, the phenylalanine residue of the DFG motif overlaps with bound AMPNP (magenta) from the active structure of EGFR. For LMTK3 the equivalent tyrosine overlaps the adenine ring of AMPPNP. **(E)** Pymol cartoon showing the packing of Tyr 314 in inactive LMTK3. Residues are colored to highlight specific features. Green, DYG motif; yellow, Lysine residue able to form the lysine-glutamate salt bridge; cyan, gatekeeper methionine; gold, residues forming a hydrophobic pocket into which Tyr314 packs and blue dashes, hydrogens bonds. In LMTK3 the Tyr314 of the DYG motif is pointing away from the active site and past the Gatekeeper residue, Met239, where it stacks between Val191 and Leu302. The hydroxyl residue of Tyr314 forms a hydrogen bond, via a water molecule, with main-chain carbonyl of Met239, and direct hydrogen bonds with the main-chain carbonyl of Glu240 and the main-chain amide of Cys242. It is thus reasonable to assume that stabilization of LMTK3 in the DYG-out, inactive state is mediated through these interactions, in a similar fashion as recently demonstrated for LRRK2 that has a tyrosine at this position too (*74*). **(F)** Pymol cartoon showing packing interactions of the HSD and DYG motif. Asn300 (cyan stick) forms a central hub around which the DYG (green sticks) and HSD motifs (white sticks) pack; red spheres, water molecules; blue dashes, hydrogen bonds. Other amino acid residues colored either as yellow sticks for clarity. In the inactive state Asn300 is hydrogen bonded to both the aspartate of the DYG motif and the histidine and aspartate of the HSD motif. The aspartate side-chain of the HSD motif is also hydrogen bonded to the hydroxyl side chain of Tyr325 and to one of the side-chain amine groups of Arg 299. **(G)** Pymol cartoon showing the packing

interaction of potential phospho-tyrosine residues. Green sticks, potential phosphotyrosine amino acid residues; yellow sticks other amino acid residues; red spheres, water molecules and blue dashes, hydrogen bonds. Tyr321 is packed against the aliphatic side chain of Lys 248 and remains partially exposed to solvent. The hydroxyl group of Tyr321 makes hydrogen bond contacts to the main-chain amide of Arg249 and the carboxyl oxygens of Asp246. In contrast, Tyr325 is less exposed and packed into a hydrophobic pocket lined by His318, Pro335 and the aliphatic side-chain of Asp324. The hydroxyl of Tyr325 forms hydrogen bonds with both the amide and to one of the nitrogen amines of the side chain of Arg299, and with the side-chain carboxyl of Asp295. Unlike, the other tyrosine residues, Tyr326 is completely exposed to solvent.

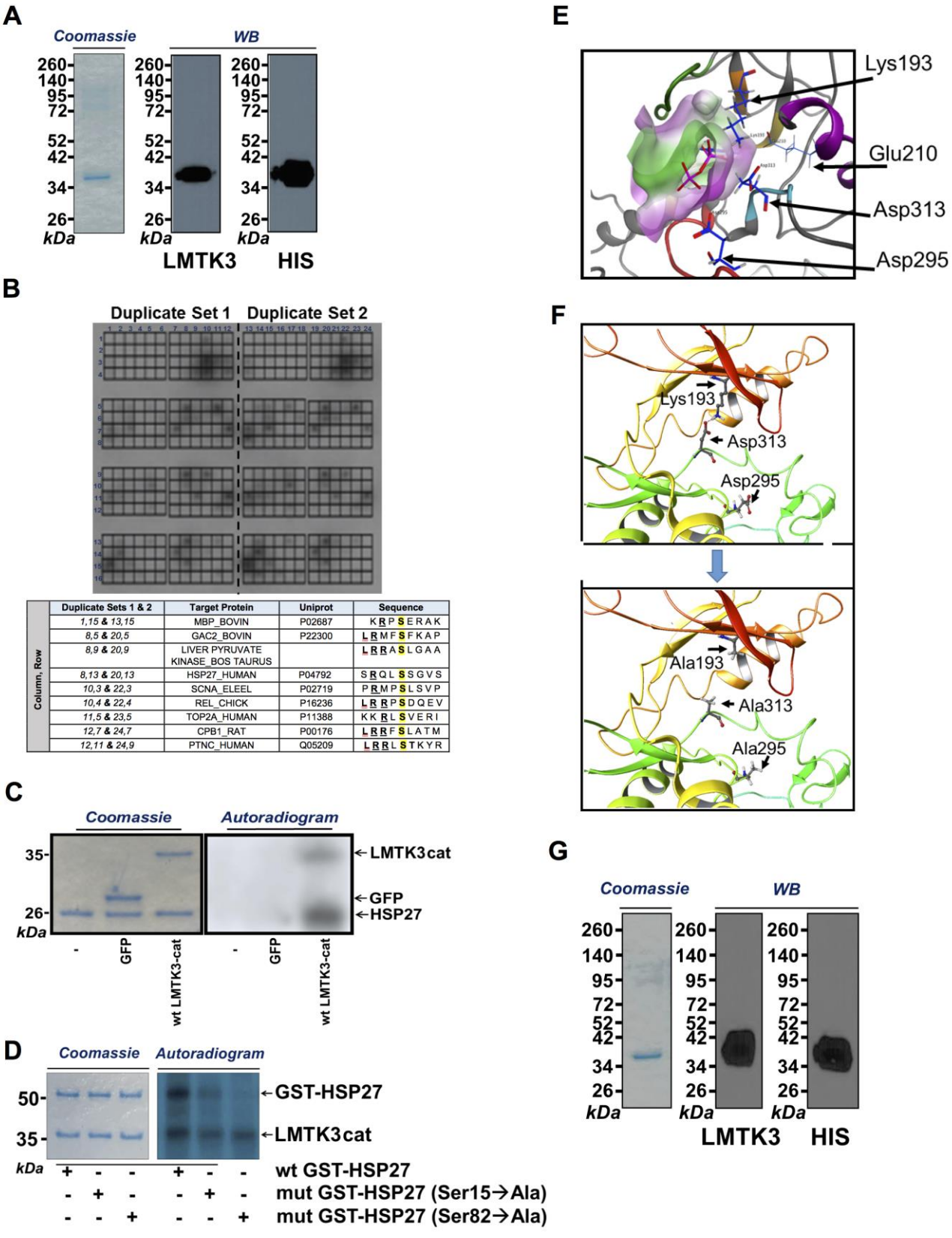
A
Coomassie
WB
260
140
95
72
52
42
34
26
kDa
LMTK3
HIS
B
Duplicate Set 1
Duplicate Set 2
Column, Row
Duplicate Sets 1 & 2 | Target Protein | Uniprot | Sequence
1,15 & 13,15 | MBP_BOVIN | P02687 | KRPSERAK
8,5 & 20,5 | GAC2_BOVIN | P22300 | LRMFSFKAP
8,9 & 20,9 | LIVER PYRUVATE KINASE_BOS TAURUS | | LRRASLGAA
8,13 & 20,13 | HSP27_HUMAN | P04792 | SRQLSSGVS
10,3 & 22,3 | SCNA_ELEEL | P02719 | PRMPSLSVP
10,4 & 22,4 | REL_CHICK | P16236 | LRRPSDQEV
11,5 & 23,5 | TOP2A_HUMAN | P11388 | KKRLSVERI
12,7 & 24,7 | CPB1_RAT | P00176 | LRRFSLATM
12,11 & 24,9 | PTNC_HUMAN | Q05209 | LRRLSTKYR
C
Coomassie
Autoradiogram
35
26
kDa
LMTK3cat
GFP
HSP27
-
GFP
wt LMTK3-cat
D
Coomassie
Autoradiogram
50
35
kDa
GST-HSP27
LMTK3cat
wt GST-HSP27
mut GST-HSP27 (Ser15→Ala)
mut GST-HSP27 (Ser82→Ala)
E
Lys193
Glu210
Asp313
Asp295
F
Lys193
Asp313
Asp295
Ala193
Ala313
Ala295
G
Coomassie
WB
LMTK3
HIS

Figure S3. Generation of catalytically active and inactive recombinant HIS-tagged LMTK3 proteins.

(A) Recombinant wt LMTK3 protein (LMTK3cat) encompassing aa 134-444, which includes the kinase domain, was prepared as described in materials and methods. A representative coomassie gel followed by western blotting detection with either LMTK3 or HIS-tag antibody is shown. **(B)** PepChip microarray slide, containing a duplicate set of peptides, was incubated with LMTK3cat in the presence of radiolabeled ATP. Peptides phosphorylated on the PepChip were visualized by autoradiography. A table with the highest phosphorylated peptides (based on the intensity/signal of the spots detected in the slide) along with their amino acids sequence is shown (the respective phosphorylated residue is highlighted in yellow). **(C)** Radiolabeled *in vitro* kinase assays using recombinant GST-HSP27 protein as a substrate and LMTK3cat as source of enzyme activity (GFP protein was used as a negative control). **(D)** Radiolabeled *in vitro* kinase assays using wt GST-HSP27, or mut GST-HSP27/Ser15Ala, or mut GST-HSP27/Ser82Ala proteins as substrates and LMTK3cat as source of enzyme activity. **(E)** LMTK3 binding pocket, with ATP (migrated from 1ATP/1IR3) and suitably relaxed (AMBER12:EHT, R-Field Solvation). It is visually clear how Lys193, Asp295 and Asp313 all surround the phosphate region of the ATP, with Lys193 binding directly to it and creating a hydrogen bond to E210 (which is commonly documented). Mutating these residues to alanine will not only destabilize ATP binding, but also change the nature of the catalytic domain from polar to non-polar (shown in the surface illustration: purple being polar, green being non–polar). **(F)** Kinase dead variation of LMTK3 where catalytic residues Lys193, Asp295 and Asp313 mutated to Ala are shown. **(G)** Recombinant mutant type LMTK3 protein (LMTK3cat-KD) encompassing aa 134-444, baring the following mutations Lys193Ala, Asp295Ala and Asp313Ala, was prepared as described in materials and methods. A representative coomassie gel followed by western blotting detection with either LMTK3 or HIS-tag antibody is shown.

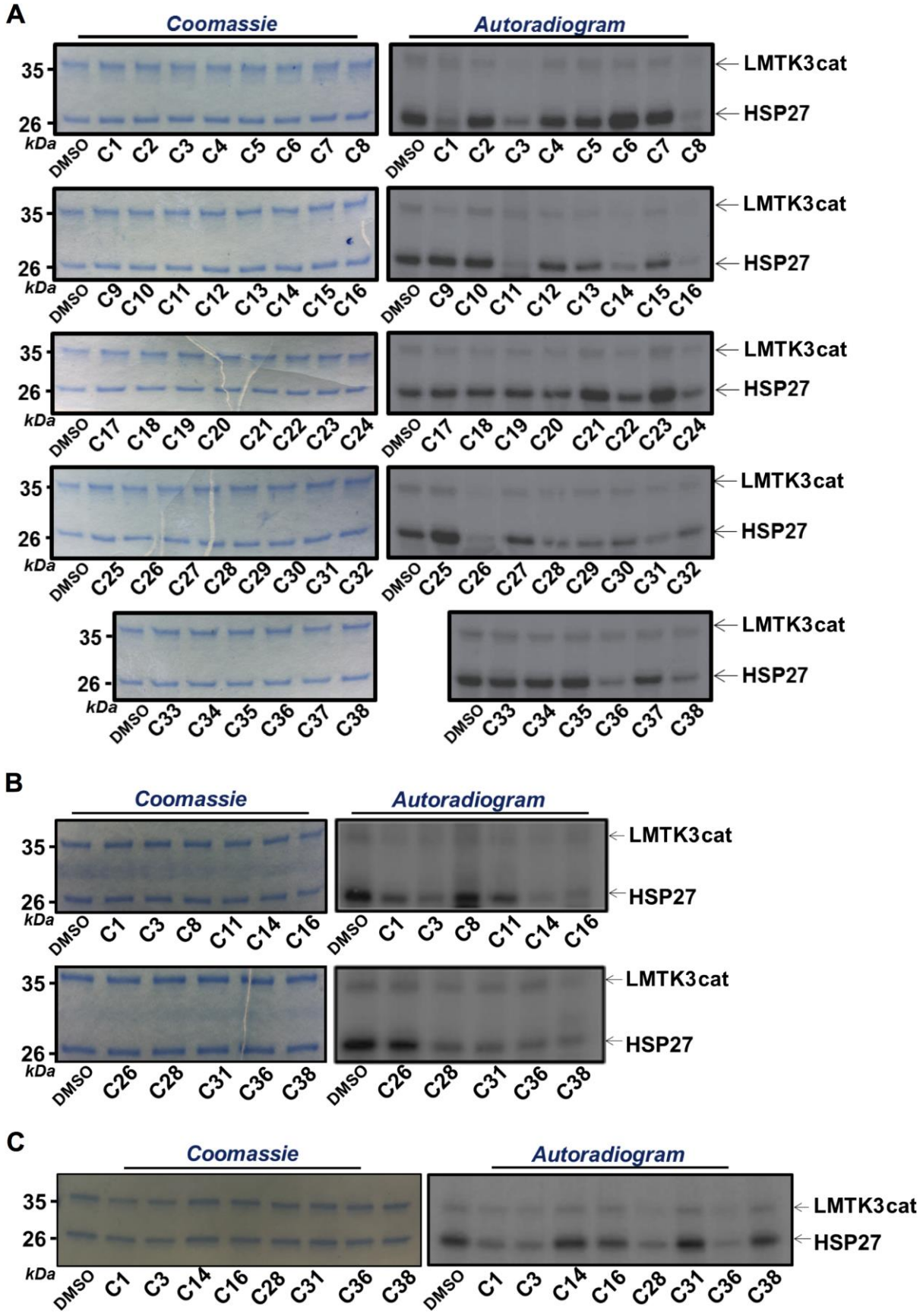
A
Coomassie
Autoradiogram
35
26
kDa
LMTK3cat
HSP27
DMSO C1 C2 C3 C4 C5 C6 C7 C8
DMSO C9 C10 C11 C12 C13 C14 C15 C16
DMSO C17 C18 C19 C20 C21 C22 C23 C24
DMSO C25 C26 C27 C28 C29 C30 C31 C32
DMSO C33 C34 C35 C36 C37 C38
B
Coomassie
Autoradiogram
DMSO C1 C3 C8 C11 C14 C16
DMSO C26 C28 C31 C36 C38
C
Coomassie
Autoradiogram
DMSO C1 C3 C14 C16 C28 C31 C36 C38

Figure S4. Determining the IC_{50} values of a panel of kinase inhibitors against LMTK3 by *in vitro* kinase assay.

(A) Radiolabeled *in vitro* kinase assays testing the ability of 38 compounds to inhibit the phosphorylation of HSP27 by LMTK3cat at 10μM. **(B)** The compounds that demonstrated >50% reduction were tested at 1 μM and the top hits were further examined at **(C)** 500 nM.

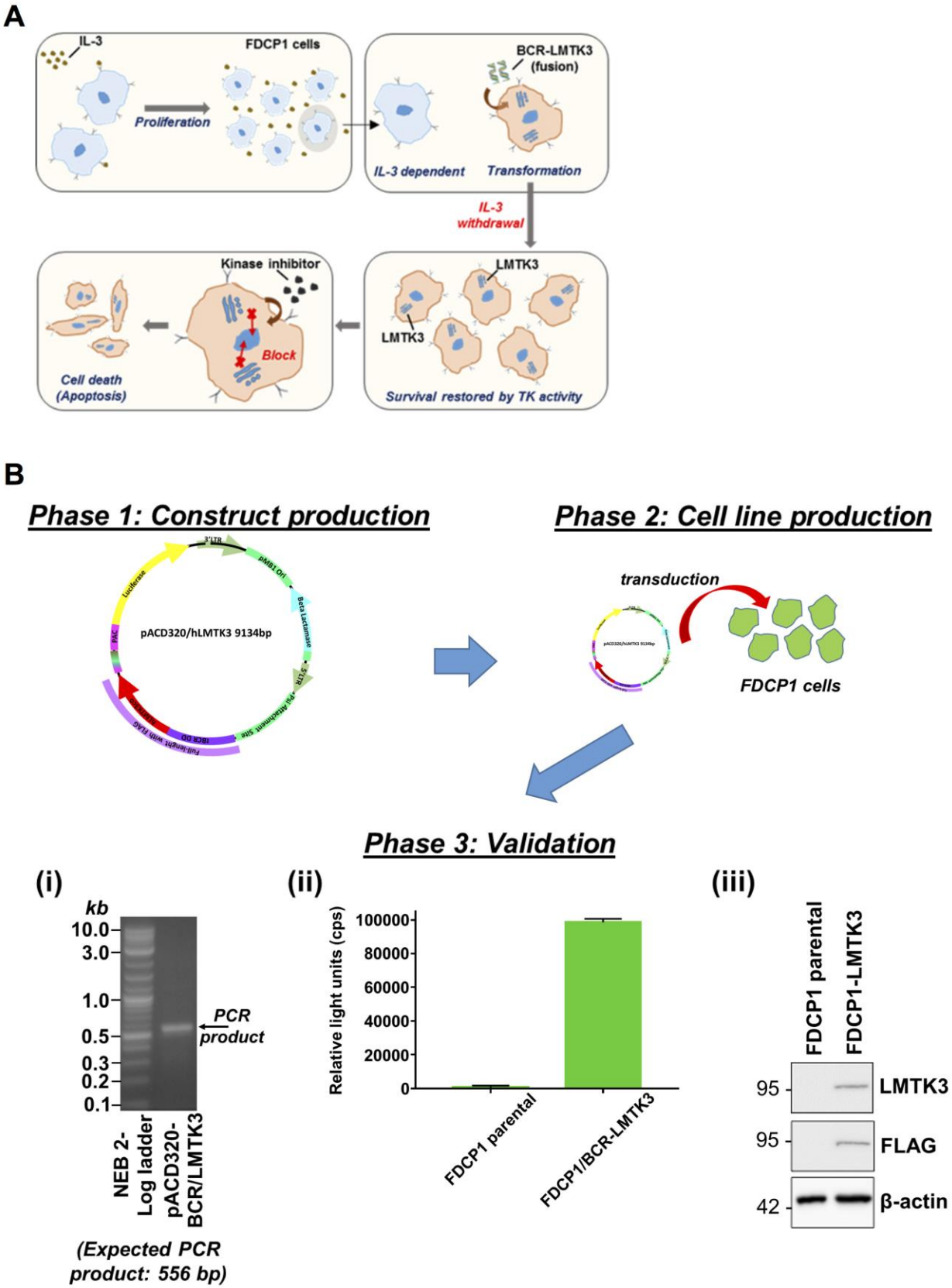
A
IL-3
FDCP1 cells
Proliferation
BCR-LMTK3
(fusion)
IL-3 dependent
Transformation
IL-3
withdrawal
Kinase inhibitor
LMTK3
LMTK3
Block
Cell death
(Apoptosis)
Survival restored by TK activity
B
Phase 1: Construct production
Phase 2: Cell line production
pACD320/hLMTK3 9134bp
transduction
FDCP1 cells
Phase 3: Validation
(i)
kb
10.0
3.0
1.0
0.5
0.3
0.2
0.1
PCR
product
NEB 2-
Log ladder
pACD320-
BCR/LMTK3
(Expected PCR
product: 556 bp)
(ii)
Relative light units (cps)
100000
80000
60000
40000
20000
0
FDCP1 parental
FDCP1/BCR-LMTK3
(iii)
FDCP1 parental
FDCP1-LMTK3
95
LMTK3
95
FLAG
42
β-actin

Figure S5. Generation and confirmation of a transformed FDCP1-LMTK3 cell line.

(A) Schematic workflow of FDCP1-LMTK3 cell line generation. **(B)** *Phase 1 (Construct production):* The LMTK3 gene (encompassing amino acids 134-444) was codon optimized and cloned into pACD320 vector and restriction digest verified. The vector included BCR fusion partner that is used to drive constitutive activation. *Phase 2 (Cell line Production):* The construct was then transduced into mouse FDCP1 cells**.** *Phase 3 (Validation):* Validation included: (i) Evaluating production of recombinant message encoding the target kinase. Functional luciferase (a passenger gene in the pACD320 construct) and kinase domain fusion proteins were produced from a bicistronic message using an intra-ribosomal entry site (IRES). This message was detected by RT-PCR using a primer set targeting the centre of the LMTK3 synthetic gene fragment (sense primer) and the 5' end of the PAC gene (antisense primer). (ii) Monitoring luciferase activity (a passenger gene in pACD320 construct). Luciferase enzymatic activity was assessed by plating 50,000 cells/well of a 384-well plate followed by detection with Bright-Glo substrate (Promega) according to the manufacturer's instructions. Data were collected in triplicate and the standard deviation determined. (iii) Western blotting demonstrating the expression of LMTK3 in FDCP1-LMTK3 cells when compared to the parental FDCP1 cell line.

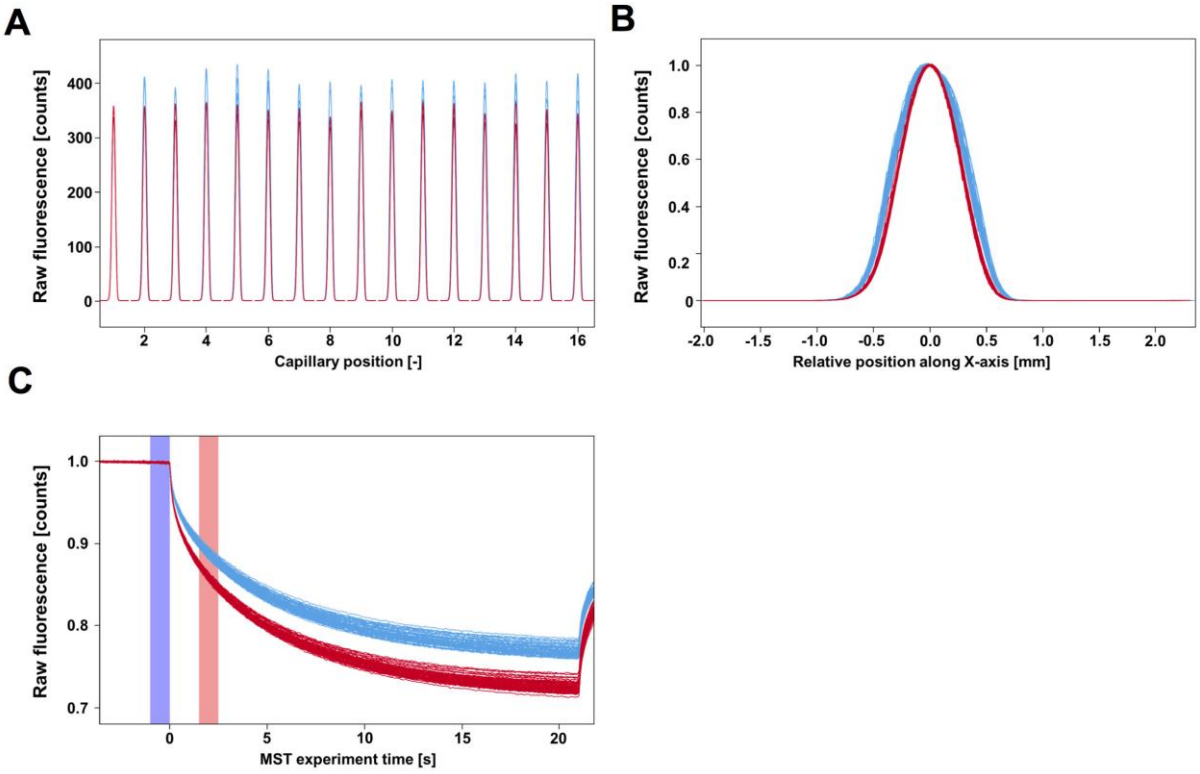

Figure S6. MST experiments demonstrating a direct interaction between LMTK3cat and CDC37.

(A) Overlaid capillary scans showing consistent fluorescence intensity measurements across capillaries containing increasing concentrations of CDC37 (blue) or Cdc37 + CDC37 (red) measured at 20% excitation power. **(B)** Overlay of capillary scans showing no adsorption of LMTK3cat to the capillary walls on addition of increasing concentrations of CDC37 (blue) or CDC37 + C28 (red). **(C)** Raw MST data collected measuring NT647-LMTK3cat thermophoresis with increasing CDC37 (blue) or CDC37 + C28 (red) concentrations. No aggregation is observed except in position 1 (10 µM CDC37); this data set has been removed from further analysis. Data collected at 60% MST power. Cold (blue) and hot (red) regions used for data analysis are highlighted.

.

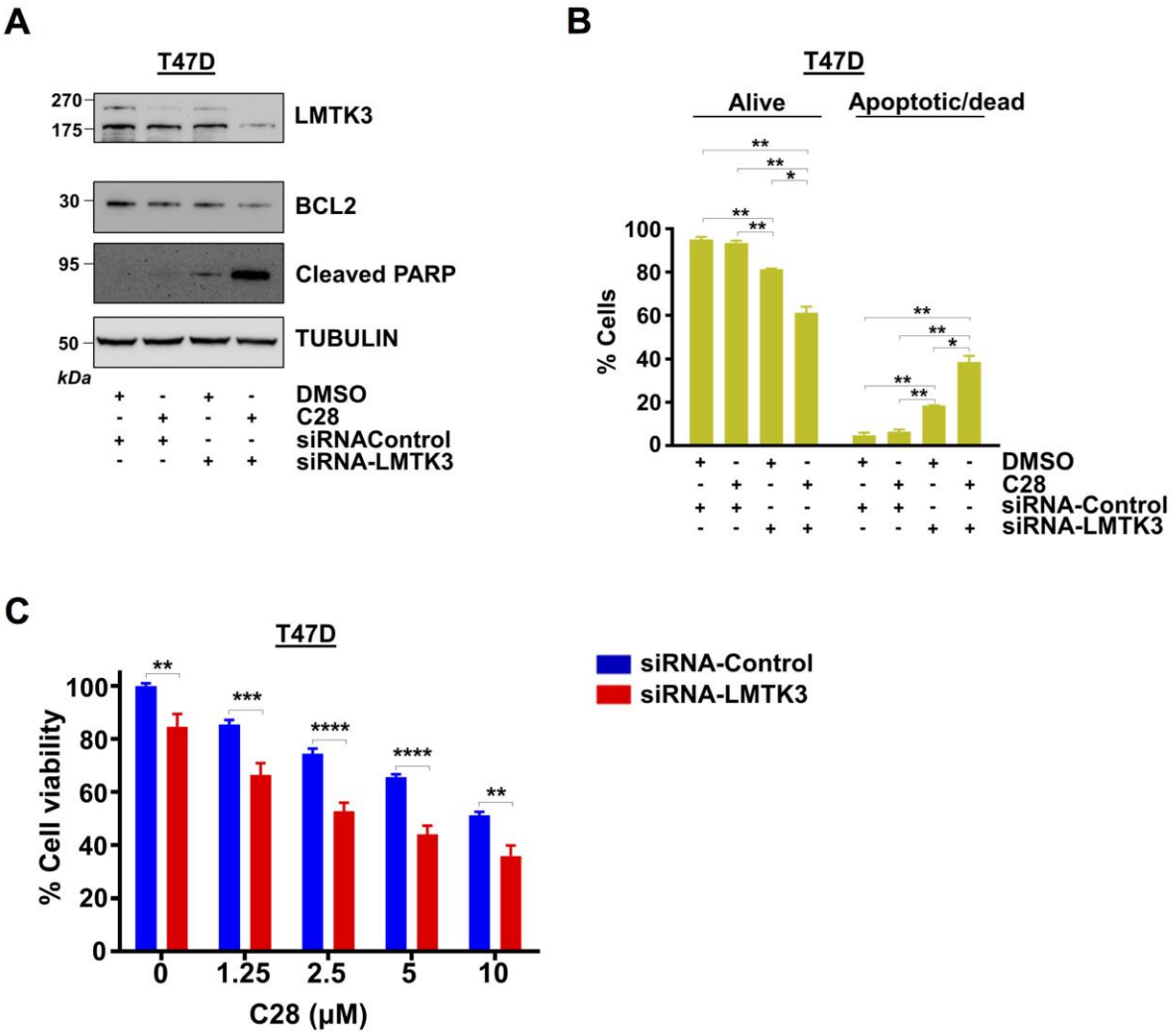

Figure S7. Effects of combined genetic or pharmacological inhibition of LMTK3.

(**A**) Western blotting analysis of BCL2 and cleaved PARP levels in T47D cells transfected with siRNA-Control or siRNA-LMTK3 for 72 h followed by treatment with 10μM of C28 for 72 h. Tubulin was used as loading control. (**B**) T47D cells were transfected with siRNA-Control or siRNA-LMTK3 for 72 h followed by treatment with 10μM of C28 for 72 h and the percentage of apoptotic and dead cells were analyzed by Annexin-V and 7-AAD staining. Unpaired t-test was performed using Prism 8 software. Results are expressed as mean ± SEM; * $P < 0.05$, ** $P < 0.01$. Each experiment was conducted at least two times. (**C**) Viability of T47D cells transfected with siRNA-Control or siRNA-LMTK3 for 72 h followed by treatment with increasing concentrations (0, 1.25, 2.5, 5 and 10 μM) of C28 for 72 h. 2-way Anova test was performed using Prism 8 software. Results are expressed as mean ± SEM; * $P < 0.05$, ** $P < 0.01$, *** $P < 0.001$, **** $P < 0.0001$. Each experiment was conducted at least two times.

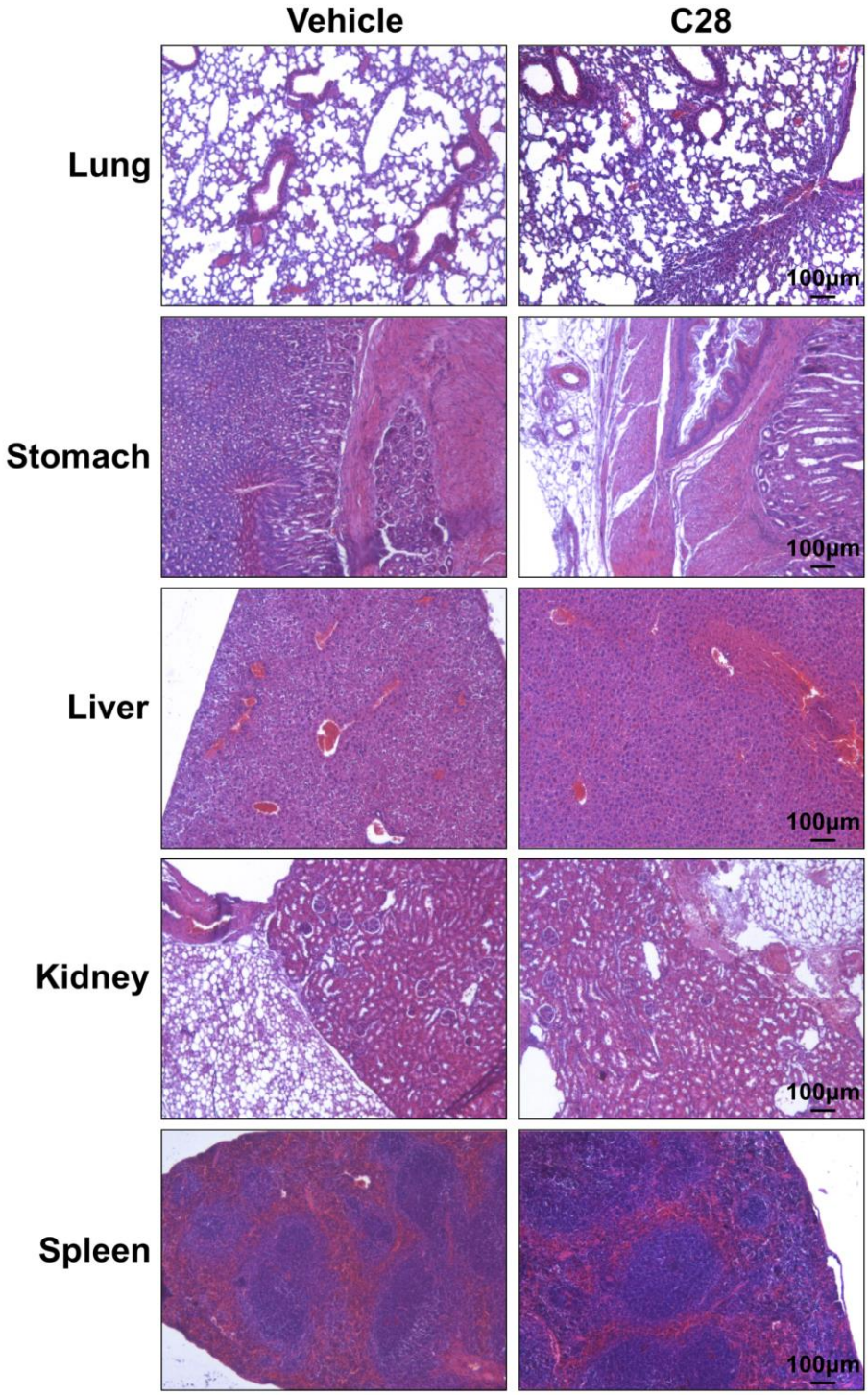

Figure S8. Histopathological findings off MMTV-Neu mice treated perorally with the C28 inhibitor.

Representative images of hematoxylin and eosin staining of sections from major organs from MMTV-Neu animals that were treated with either vehicle or C28 (10 mg/kg). Original magnification, 10×. Scale bar, 100 μm.

Supplementary Tables

Table S1. Crystallization statistics.

Attached as separate excel file.

Table S2. SILAC data.

Attached as separate excel file.

Table S3. HTRF screening data.

Attached as separate excel file.

Table S4. Radioactive filter binding and active site-directed competition binding assays selectivity data.

Attached as separate excel file.

Table S5. Antiproliferative activity of C28 across the NCI-60 cell lines.

Attached as separate excel file.

Table S6. Antitumor activity of C28 in transgenic and xenograft mice models.

Attached as separate excel file.